Hair-Follicle Mesenchymal Stem Cell Activity during Homeostasis and Wound Healing

Emil Aamar[1], Efrat Avigad Laron[1], Wisal Asaad[1], Sarina Harshuk-Shabso[1] and David Enshell-Seijffers[1]

The mesenchymal components of the hair follicle—the dermal papilla (DP) and dermal sheath (DS)—are maintained by hair follicle dermal stem cells, but the position of this stem cell population throughout the hair cycle, its contribution to the maintenance of the dermis, and the existence of a migratory axis from the DP to the dermis remain unclear. In this study, we show that during homeostasis DP and DS cells are confined to their compartments, and during the regression phase of the hair cycle, some DP/DS cells undergo apoptosis and subsequently are internalized by nearby adipocytes. In contrast, during wound healing, DP/DS cells move toward the wound but do not directly participate in follicle neogenesis. Furthermore, hair follicle dermal stem cells, driving the cyclic renewal of the DS during the hair cycle, are heterogeneous and are housed during the growth phase within the most proximal part of the DS. Our analysis provides insight into the mechanisms of tissue maintenance and reveals a potential function of adipocytes in phagocytosis.

Journal of Investigative Dermatology (2021) **141,** 2797–2807; doi:10.1016/j.jid.2021.05.023

INTRODUCTION

Hair follicles (HFs) undergo cycles of growth (i.e., anagen), destruction (i.e., catagen), quiescence (i.e., telogen), and regeneration (Botchkarev and Kishimoto, 2003; Millar, 2002; Stenn and Paus, 2001). During anagen, concentric layers of epithelial cells that include the hair shaft, the inner root sheath, and the outer root sheath constitute the mature HF (Stenn and Paus, 2001). At the base of the follicle, a mesenchymal group of cells known as the dermal papilla (DP) is embedded in the hair bulb and is surrounded by proliferating keratinocytes collectively called matrix progenitor cells (Legué and Nicolas, 2005). The DP regulates the duration of hair growth by orchestrating the activity and behavior of the overlying matrix progenitor cells (Enshell-Seijffers et al., 2010a; Harshuk-Shabso et al., 2020). Toward the end of the anagen phase, the DP dampens the activity of matrix cells, and consequently, proliferation in the hair matrix ceases (Harshuk-Shabso et al., 2020). Differentiation of some cells within the matrix forms the terminal structure of the hair club, while the rest of the matrix cells undergo programmed cell death as the catagen phase ensues (Ito et al., 2004). During the catagen phase, the majority of the lower outer root sheath undergo apoptosis, while the follicle regresses (Mesa et al., 2015). Consequently, cells within the upper outer root sheath collapse around the proximal end of the hair and form the bulge region and the secondary germ (Hsu et al., 2011; Ito et al., 2004). The DP survives the apoptotic milieu and is drawn up with the regressing epithelial strand to lie beneath the secondary germ. A quiescent phase of variable length precedes the induction of a new cycle and regeneration of the lower follicle. Both anagen induction and regeneration require the inductive and instructive activity of the DP (Avigad Laron et al., 2018; Chi et al., 2013; Enshell-Seijffers et al., 2010a; Rompolas et al., 2012).

An additional mesenchymal component of the HF is a thin layer of dermal sheath (DS) cells that encapsulates the HF during the anagen phase (Jahoda, 2003; Martino et al., 2021) and plays an important role in follicle regression (Heitman et al., 2020). This DS compartment is classified into two domains: the DS cup (DSC) that surrounds the bulb region and the distal DS (DDS) that encloses the outer root sheath up to the bulge region (McElwee et al., 2003). During catagen, DS cells in both compartments undergo apoptosis. Few DS cells survive, and during telogen, these preserved DS cells reside at the periphery of the DP (Rahmani et al., 2014). At anagen onset, these DS cells proliferate to reconstitute the DS compartment. Cell lineage analysis of DS cells clearly demonstrated that the cyclic expansion and reduction of the DS compartment require the presence of DS mesenchymal stem cells, termed HF dermal stem cells (hfDSCs), which are able to self-renew and regenerate the DS compartment (Rahmani et al., 2014).

In contrast to the DS compartment, very little proliferation or apoptosis is observed within the DP (Tobin et al., 2003a, 2003b). Yet, DP cell number fluctuates substantially during the hair cycle, peaking at mid anagen and declining by half during the transition from anagen to telogen (Tobin et al., 2003a). Cell immigration and emigration between the DS and DP compartments during the hair cycle has been shown mostly in depilation experiments to account at least in part for this fluctuation of DP size (Chi et al., 2010; Rahmani et al., 2014; Tobin et al., 2003a, 2003b). Whereas hfDSCs during early anagen contribute new cells to the DP in addition to regenerating the DS, DS-recruited DP cells during catagen have been suggested to segregate from the DP and

[1]*The Laboratory of Developmental Biology, The Azrieli Faculty of Medicine, Bar-Ilan University, Safed, Israel*

Correspondence: David Enshell-Seijffers, The Laboratory of Developmental Biology, The Azrieli Faculty of Medicine, Bar-Ilan University, 8 Henrietta Szold, Safed, 1311502, Israel. E-mail: david.enshell@biu.ac.il

Abbreviations: aSMA, alpha-smooth muscle actin; DDS, distal dermal sheath; DP, dermal papilla; DS, dermal sheath; DSC, dermal sheath cup; HF, hair follicle; hfDSC, hair follicle dermal stem cell; P, postnatal day

Received 31 October 2020; revised 10 May 2021; accepted 11 May 2021; accepted manuscript published online 22 June 2021; corrected proof published online 14 September 2021

reintegrate within the telogen DS stem cell niche (Rahmani et al., 2014). However, the extent to which this bidirectional migration accounts for the extensive fluctuation of DP cell number during the hair cycle remains unclear. Intriguingly, microscopy analysis previously revealed that some DS cells detach from the follicle during catagen (Tobin et al., 2003a), suggesting that stem cells within the mesenchymal compartments of the follicle contribute to the maintenance of the dermis during homeostasis and that a unidirectional trajectory of migration and transdifferentiation from DP to DS to dermis may also occur (Jahoda, 2003). In support of these hypotheses, cell lineage analysis of DS cells using the alpha-smooth muscle actin (aSMA)-creRT2 mouse line has recently suggested that hfDSCs contribute new fibroblasts to the dermis and that this contribution is further exacerbated when β-catenin is forcedly activated in the DS (Tao et al., 2019). In contrast, other studies that label DS cells, either by the same aSMA-creRT2 mouse line or by the Acan-creER mouse line, did not report the detection of such contribution (González et al., 2017; Heitman et al., 2020; Rahmani et al., 2014; Shin et al., 2020), challenging its occurrence. Furthermore, cell lineage analysis of DP cells, using the Prom1-creRT2 mouse line, suggested that during homeostasis, DP cells remain confined to the DP compartment (Kaushal et al., 2015). However, the partial labeling of the DP compartment, which is intrinsic to the method used in that study, and the cellular heterogeneity within the DP (Yang et al., 2017) preclude the adequate analysis to test unequivocally the contribution of the DP to the maintenance of the dermis during homeostasis.

The physical proximity of hfDSCs to the DP during telogen allows hfDSCs to bipotently contribute to both the DS and DP during early anagen (Rahmani et al., 2014). However, the morphological reorganization of the HF during regeneration requires the relocation of these hfDSCs and concomitantly the maintenance of their stemness. Clonal analysis of DS cells suggested that whereas hfDSCs reside within the periphery of the DP during telogen, during anagen, this stem cell population is relocated to surround the hair bulb and reside within the DSC (Rahmani et al., 2014). However, the method used in that study to label the DS compartment did not distinguish between the DDS and DSC, and therefore, the location of hfDSCs in the DSC during anagen could not be tested directly. In this study, we have generated a mouse line that allows the specific labeling of DP and DSC cells to fate map their lineages during homeostasis and wound repair.

RESULTS

DP and DS cells are confined to the mesenchymal compartments of the HF during homeostasis

To endogenously label cells within the DP and DSC in an inducible manner, the *Corin* locus that is expressed specifically in the DP and DSC during the anagen phase of the hair cycle (Enshell-Seijffers et al., 2008, 2010b) was exploited to generate a knock-in mouse line (i.e., Corin-CreRT2) that expresses the tamoxifen-inducible cre recombinase (i.e., CreRT2) in the DP and DSC. For lineage tracing, mice homozygous for the *Corin-CreRT2* allele and heterozygous for the *r26EGFP* reporter allele (Madisen et al., 2010) were generated and administered with tamoxifen. Tamoxifen was intraperitoneally injected during the early anagen of the first cycle once a day for 3 days (on postnatal day [P] 8, P9, and P10) (Figure 1a). To test the labeling efficiency, injected mice were harvested on P12, 2 days after the last injection (Figure 1b). In contrast to the partial labeling of DP cells by the Prom1-creRT2 mouse line (Kaushal et al., 2015), all DP cells in all follicles were apparently GFP labeled. In addition, partial labeling was observed in the DSC. As expected, no label was found in other parts of the dermis or in the epithelial compartment. Furthermore, no GFP labeling was found in littermate controls injected with a vehicle without tamoxifen (Figure 1c), demonstrating that the CreRT2 in the Corin-CreRT2 line has no tamoxifen-independent activity.

Tamoxifen-injected mice were followed for five subsequent hair cycles (Figure 1a). Whereas the first and second hair cycles are highly synchronized, anagen induction of the third and later cycles is stochastic and occurs in patches (Plikus et al., 2008). Furthermore, in contrast to the telogen of the first cycle that lasts for a few days, the telogen duration of the second and later cycles varies substantially between mice and persists for weeks or even months (Plikus et al., 2008). To overcome the very long telogen of the second cycle and the unsynchronized nature of the following cycles, anagen was artificially induced by depilation 1 week after the follicles entered the telogen phase of the second and subsequent cycles. Mice were depilated repeatedly three times to complete altogether five cycles (Figure 1a). At the telogen of the first cycle (Figure 1d), GFP-positive cells were observed as a single group of cells at the bottom of the telogen follicle and were completely absent from the upper interfollicular dermis (papillary dermis). Furthermore, immunostaining with anti-ITGA8, a marker for telogen DS (Rahmani et al., 2014), illustrates the presence of labeled DS cells lining the DP (Figure 1e), suggesting that some DSC cells survive the catagen phase and relocate to envelope the DP during telogen. This restricted labeling of GFP to the DP and DS compartments persisted even after five hair cycles (Figure 1f). To exclude the confounding effects that might be caused by depilation and to trace the DP/DS fate map throughout the mouse life span under physiological conditions, tamoxifen-injected, undepilated mice aged 25 months at telogen were also analyzed. Similarly, GFP expression was confined only to the DP and DS (Supplementary Figure S1a). Together, these data suggest that DP and DS cells during homeostasis are committed to their compartments, that they physically constitute a single mesenchymal entity, and that they do not migrate to repopulate the dermis or to transdifferentiate to other types of mesenchymal cells.

Apoptotic cells within the DS/DP compartment during the regression phase are internalized by adipocytes

In contrast to the papillary dermis, GFP labeling was observed during telogen within the dermis in a very restricted plane beneath the zone of the HFs called panniculus adiposus (Figure 1d). However, this GFP labeling at the panniculus adiposus did not resemble coherent whole cells but instead appeared more like fragments of apoptotic cells. To track the formation of these GFP-labeled cell fragments, TUNEL staining was performed during the catagen of the first

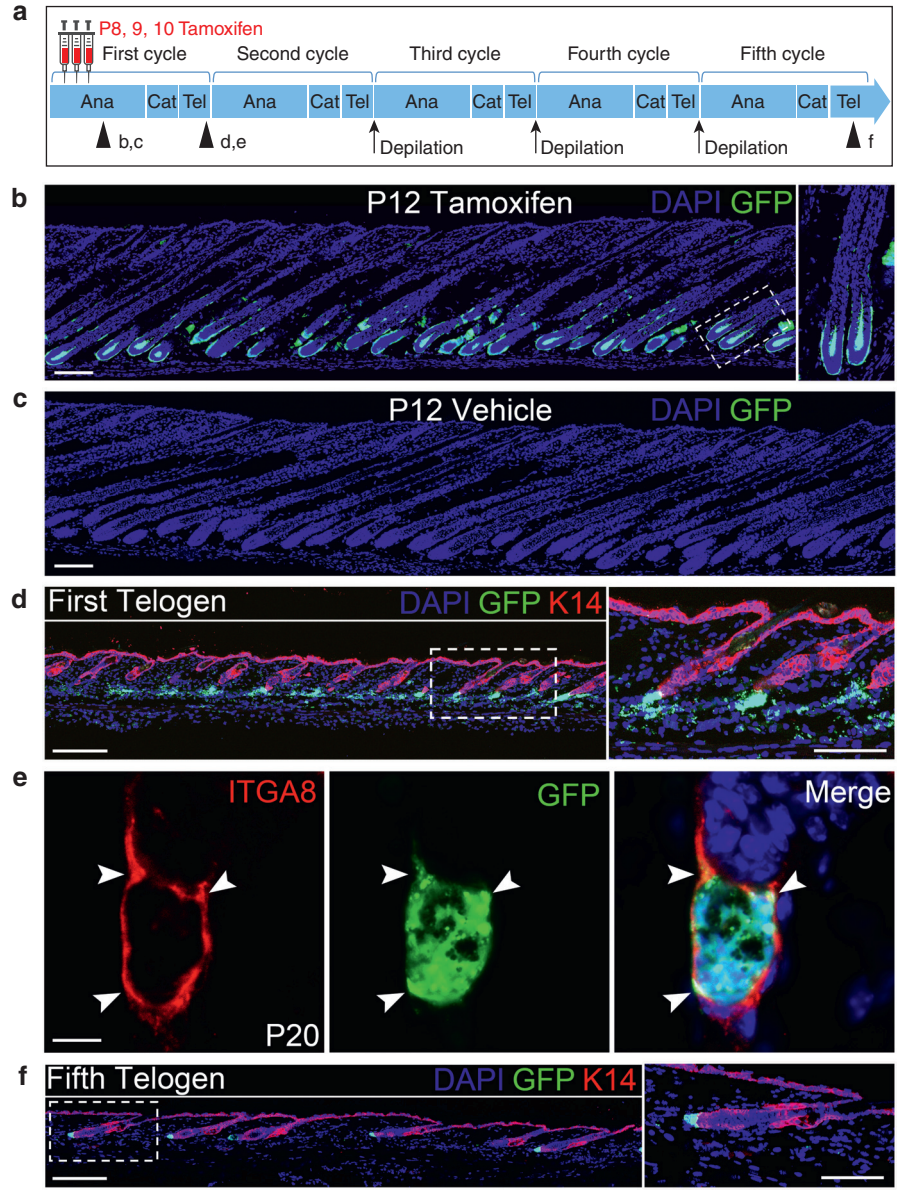

Figure 1. DP and DSC cells do not migrate from their compartments to other parts of the dermis. (**a**) Schematic representation of the experimental protocol over multiple and consecutive hair cycles. Above, the times of tamoxifen injection (red syringes) are shown. Below, arrows indicate the times of depilation, and arrowheads mark the times of skin collection with a reference to the figure panels showing the relevant skin sections and analysis. (**b, c**) Skin sections of (**b**) tamoxifen- and (**c**) vehicle-injected mice, 2 days after the last injection. Note that all DP cells and most DSC cells are GFP labeled (green) in the tamoxifen-injected mouse, whereas no labeling is observed in the control. The panel on the right side in **b** shows a higher magnification of the field enclosed by the white dashed rectangle. n = 5 mice for vehicle and n = 5 mice for tamoxifen injected. Bar = 200 μm. (**d**) A skin section of a tamoxifen-injected mouse showing the cell fate of GFP-labeled cells at the telogen of the first cycle. The panel on the right side shows a higher magnification of the field in the white dashed rectangle to illustrate that DP and DS cells constitute a single compartment during telogen and that no migration from this compartment to other parts of the upper dermis occurs during the first cycle. However, note that GFP-labeled fragments in the panniculus adiposus are observed (see text). n = 5 mice. Bar = 200 μm on the left and 100 μm on the right. (**e**) A telogen follicle on P20 (first cycle) immunostained for ITGA8 (red) is shown to illustrate GFP-labeled DS cells. The same follicle is shown on the left, middle, and right panels. White arrowheads indicate ITGA8/GFP double-positive cells. Bar = 10 μm. (**f**) Cell lineage analysis after five hair cycles revealed similar observations. n = 3 mice. Bar = 200 μm on the left and 100 μm on the right. In **d** and **f**, the basal layer of the epidermis and the ORS of hair follicles were labeled with anti-K14 (red). Nuclei are in blue (DAPI). Sections were imaged with an upright fluorescence apotome microscope except for that in **e,** which was taken with a confocal microscope. Ana, anagen; Cat, catagen; DP, dermal papilla; DSC, dermal sheath cup; K14, keratin 14; ORS, outer root sheath; P, postnatal day.

cycle. This clearly illustrates that GFP-labeled cells undergo apoptosis (Figure 2a), consistent with the observation that DS cells undergo apoptosis during catagen (Rahmani et al., 2014). Immunostaining for mature adipocyte markers such as perilipin and caveolin revealed that these markers are colocalized with the GFP-labeled cell fragments during the transition from catagen to telogen, supporting that the GFP fragments are internalized by adipocytes (Figure 2b and Supplementary Figure S2a). This was further corroborated by Z-stack confocal analysis (Supplementary Figure S2b). Close

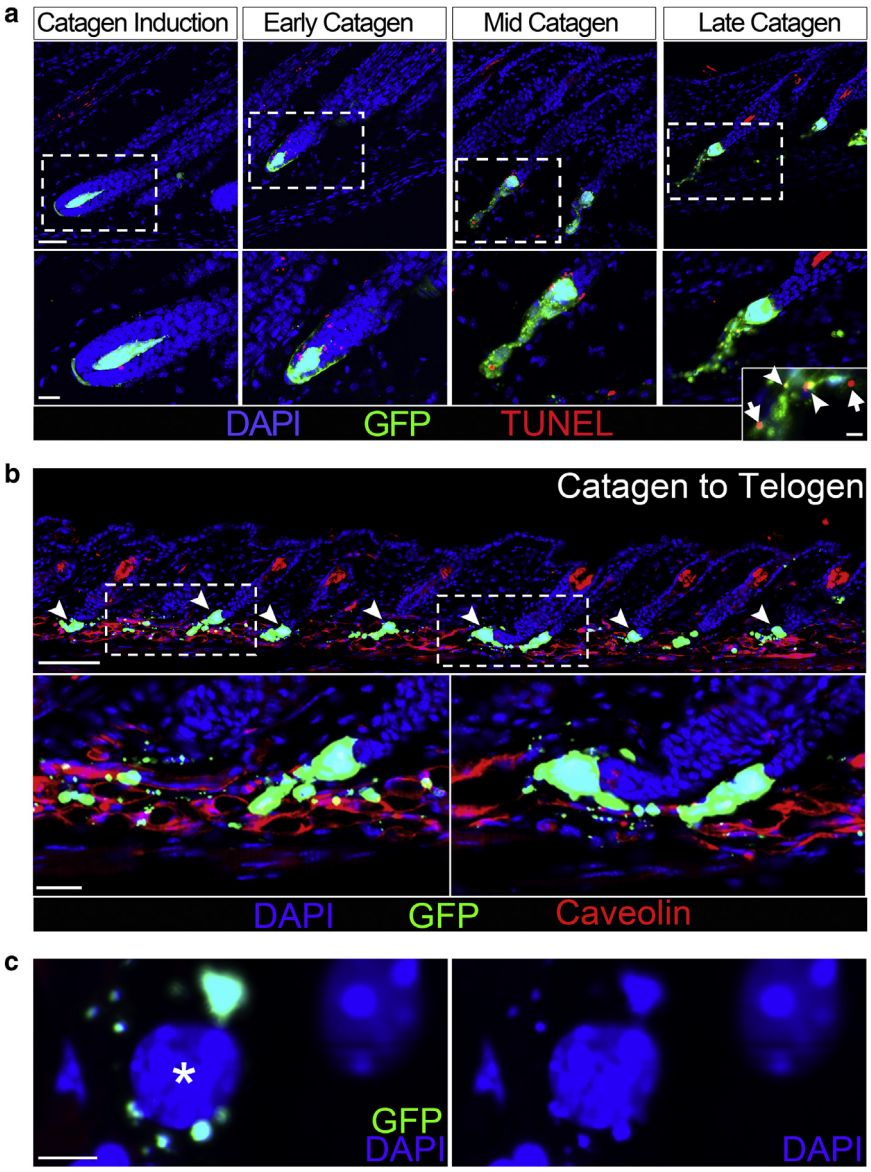

Figure 2. GFP-labeled cells undergo apoptosis during catagen and subsequently are internalized by nearby adipocytes. (**a**) TUNEL staining (red) of skin sections during the catagen of the first cycle is shown. Different HFs at distinct stages of catagen are depicted. n = 5 mice. Bar = 50 μm in the upper panels. Higher magnifications of the fields framed within the dashed white rectangles are shown in the panels below, respectively. Bar = 20 μm. Note that apoptosis is readily observed within the regressing epithelial strand throughout the catagen phase. In contrast, apoptosis within the GFP-labeled cells (green) is detected from mid catagen and only in labeled cells that lag behind the regressing DP. No TUNEL-positive stain is found in the DP. The panel in the right bottom corner is a higher magnification of a region beneath the regressing DP. Arrows indicate TUNEL-positive stain within a cloud of GFP, and arrowheads designate TUNEL and GFP colocalization. Bar = 5 μm. DAPI labels nuclei (blue). (**b**) The GFP-labeled fragments colocalize with the panniculus adiposus layer specifically labeled with anti-Caveolin (red). n = 3 mice. Bar = 100 μm. The panels below show higher magnifications of two selected fields enclosed with white dashed rectangles in the upper panel. Bar = 25 μm. Note the colocalization of some of the GFP-labeled remnants with the caveolin-stained adipocyte cells, suggesting that the fragments are being engulfed and cleared by these cells. (**c**) High magnifications of the same field with only two adipocytes are shown to illustrate that the internalized GFP-labeled fragments contain DNA, suggesting that these fragments are apoptotic bodies. On the left panel, both GFP and DAPI are shown, and on the right, only DAPI is displayed. Note the small GFP and DAPI double-positive fragments versus the big adipocyte GFP-negative DAPI-positive nucleus. The white star (asterisk) indicates the adipocyte nucleus. Bar = 5 μm. Sections were imaged with a confocal microscope except for that in **b,** which was taken with an upright fluorescence apotome microscope. DP, dermal papilla; HF, hair follicle.

inspection of the GFP fragments revealed that these labeled fragments contain DNA, suggesting that the GFP-labeled fragments are internalized apoptotic bodies (Figure 2c). Together, these data suggest that adipocytes play an important role as nonprofessional phagocytes that ingest and clear DS/DP cells undergoing apoptosis during the regression phase.

DS stem cells are relocated to and reside in the DSC during the growth phase

Previously, cell lineage analysis revealed that hfDSCs reside at the boundaries of the DP during telogen (Rahmani et al., 2014). The same analysis also suggested that the DSC compartment functions as a niche for hfDSCs during anagen. As the labeling protocol, developed in our study, allows the

GFP labeling of DS cells predominantly within the DSC compartment (Figure 1b), this hypothesis can be addressed directly. The presence of GFP-labeled cells in the DS compartment during the telogen of the first cycle indicates that DSC cells survive the apoptotic microenvironment during catagen and contribute to the formation of the DS compartment during telogen (Figure 1e). However, because the exact proportion of hfDSCs within the telogen DS remains unclear (Rahmani et al., 2014), the stemness nature of the labeled DS cells in the telogen DS found in our study is obscure. Furthermore, the DSC labeling method by the *Corin-creRT2* is only partial, and therefore, the stemness identity of the labeled DS cells in the DSC remains elusive. Because hfDSCs are the source for the expansion and reconstitution of the DS compartment during every cycle (Rahmani et al., 2014), the number of labeled DS cells during anagen outside the DSC is predicted to progressively increase from cycle to cycle if hfDSCs reside within the DSC during anagen and are labeled. To test this prediction, tamoxifen was injected during the early anagen of the first cycle when labeling is restricted to the DSC, and the presence of labeled DS cells within the DDS was followed through four successive cycles (Figure 3a). Indeed, a progressive incline of labeled DS cells from cycle to cycle was observed in the DDS compartment (Figure 3b–f and Supplementary Figure S3a–f), supporting the hypothesis that hfDSCs exchange locations during the hair cycle and are relocated from the periphery of the DP during telogen to the margins of the bulb during anagen.

Note that our experimental protocol included two rounds of depilation (Figure 3a). To exclude the possibility that the increase in GFP-labeled cells in the DDS reflects a wound response to depilation, a spontaneous anagen skin of undepilated mice aged 18 months was tested (Supplementary Figure S1b). Cross-sectional analysis through the patches of anagen skin revealed extensive GFP labeling in the DDS of anagen follicles (Supplementary Figure S1c) comparable with that in the experimental protocol with depilation. This illustrates not only that the increase of GFP labeling in the DDS is a consequence of physiological maintenance of the DS by hfDSCs but also suggests that hfDSCs are efficiently maintained throughout adult life. To directly assess the maintenance of hfDSCs during aging, the number of ITGA8 and GFP double-positive cells in the telogen DS was compared between young (aged ~2 months; second telogen) and old (aged >18 months) mice (Figure 3g and h and Supplementary Figures S1d and e and S3g). No differences in the number of double-positive cells between young and old mice were detected—neither in the proportion of follicles with labeled DS cells (which was 100% regardless of the mouse age) nor in the number of labeled DS cells per follicle (Figure 3g and h and Supplementary Figure S3g). This clearly suggests that hfDSCs are efficiently maintained during aging.

aSMA and Corin levels are heterogeneous in the DSC

Regardless of the cycle, the number of labeled DS cells was always higher in more proximal regions of the DS compartment than in distal parts, and this gradient along the proximal–distal axis progresses from cycle to cycle toward the distal end (Figure 3). Such gradient was not reported in the cell lineage tracing analysis previously performed with the aSMA-creRT2 mouse line, in which labeled DS cells were found all over the DS compartment and appeared to be distributed evenly within the middle part of the HF (González et al., 2017; Rahmani et al., 2014; Shin et al., 2020). Furthermore, although the cell lineage analysis with the aSMA-creRT2 mouse line supports a model of hfDSC exhaustion in which the number of hfDSCs declines during aging (Shin et al., 2020), our analysis suggests that hfDSCs are persistently maintained throughout adult life. To explore the underlying mechanism of these differences, the DSC labeling by the Corin-creRT2 method was further analyzed.

To determine whether the partial labeling of the DSC follows a random behavior of cre activity or may reflect a cellular heterogeneity within the DSC, Corin expression was carefully re-examined. Whereas in situ hybridization for *Corin* on P12 (Figure 4a) confirmed that *Corin* transcripts are detected only in the DP (Enshell-Seijffers et al., 2008), immunostaining for Corin (Figure 4b) reillustrated that Corin is expressed also in the DSC (Enshell-Seijffers et al., 2010b), albeit at substantially lower levels. This discrepancy between Corin in situ hybridization and immunostaining suggests that Corin expression in the DSC is too low to be detected by the former. Furthermore, by manipulating the conditions and image exposure of Corin immunostaining, the heterogeneous nature of Corin expression was revealed (Figure 4b, middle and right panels). Within the DP, Corin proteins create a gradient along the distal–proximal axis of the DP. However, within the DSC, the levels of Corin protein unorderly vary, demonstrating the presence of Corin-low and Corin-high DSC cell populations. To further corroborate this heterogeneity, we exploited the *mCherry-H2B* fluorescent gene that was also inserted into the *Corin* locus of the Corin-creRT2 line to mark DP and DSC cells in a cre-independent manner (Supplementary Figures S4 and S5). Whereas a gradient of nuclear mCherry-H2B was readily observed within the DP, nuclear mCherry-H2B in some cells of the DSC was detected only when the image is overly exposed (Supplementary Figure S5a). Furthermore, nuclear mCherry-H2B has never been found in the DDS throughout this study, further corroborating that Corin expression is restricted to the DSC.

To further explore this cell heterogeneity within the DSC, skin sections from tamoxifen-injected mice on P12 were immunostained with anti-aSMA antibodies. Consistent with previous reports, aSMA is expressed in the arrector pili muscle, blood vessels, and the DS (Figure 5a). Of note, aSMA expression within the DS was extremely high in middle parts along the follicle with asymmetric distribution toward the follicle anterior side (Figure 5a). Although this asymmetric pattern was maintained in the DSC, aSMA levels in this part of the follicle were low and heterogeneous (Figure 5b and c). Intriguingly, GFP-positive cells within the DSC were often aSMA low (Figure 5c), suggesting that *Corin-creRT2* in the DSC preferentially labels cells with low levels of aSMA. Together, these data suggest that the partial labeling of the DSC does not reflect mere inefficient labeling of the DSC and that the labeled and unlabeled cells in the DSC may reflect two distinct cell populations with different properties.

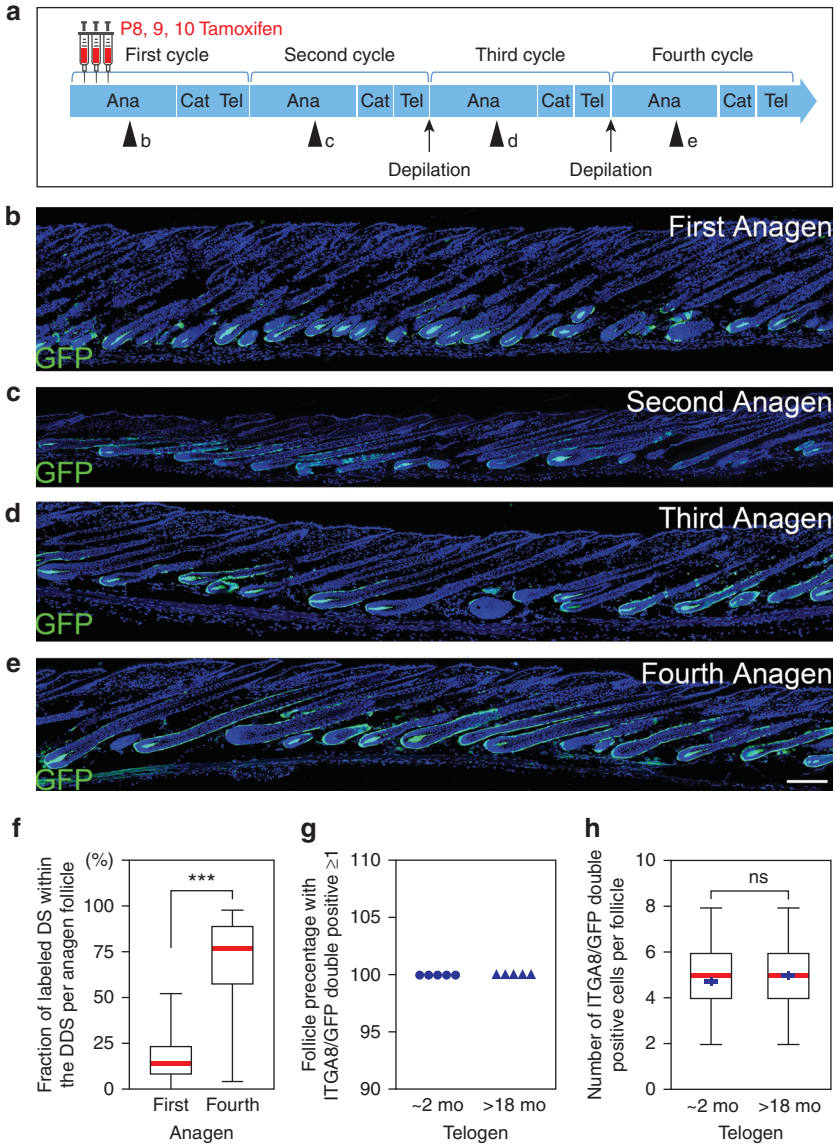

Figure 3. DS stem cells during anagen reside in the DSC. (**a**) Schematic representation of the experimental protocol over consecutive hair cycles. As before, tamoxifen injection (red syringes), depilation (arrows), and skin collection (arrowheads; with a reference to the relevant figure panels) times are shown. (**b**–**e**) Skin sections from the first to the fourth hair cycle are displayed, respectively, showing a progressive increase of the number of DS cells along the DDS part of the follicle from cycle to cycle. DAPI labels the nuclei (blue). n = 3 mice per cycle. Bar = 200 μm. (**f**) The percentage of the GFP-labeled DS versus that of nonlabeled DS per follicle during anagen is presented by box and whisker plot (red midline: median, box: 25th and 75th percentiles, whiskers: minimum and maximum). For each follicle, the GFP intensities along a fixed distance were measured on both sides, and the ratio between GFP positive and negative was calculated (see Supplementary Figure S3). n = 3 mice for each cycle, and 100 follicles per mouse were scored. Mann–Whitney test was performed. ***$P < 0.0001$. (**g**) Quantification of the percentage of follicles per mouse with at least one ITGA8/GFP double-positive cell is presented by a scatter plot to compare young mice (aged ~2 mo) at the telogen of the second cycle with old mice (aged >18 mo) in telogen. n = 5 mice per age, and at least 30 follicles per mouse were scored. (**h**) The number of labeled DS cells (ITGA8/GFP double positive) per telogen follicle in young and old mice was quantified and presented as a box and whisker plot (red midline: median, blue cross: mean, box: 25th and 75th percentiles, whiskers: minimum and maximum). n = 5 mice per age, and at least 30 follicles per mouse were scored. Mann–Whitney test was performed. Cat, catagen; DDS, distal dermal sheath; DS, dermal sheath; DSC, dermal sheath cup; mo, month; ns; not significant; P, postnatal day.

The boundaries between the mesenchymal components of the HF and the dermis are compromised during wound healing

To test whether this restriction of DP and DS cells to their follicular compartments persists also during wound healing, full-thickness back skin wounds were introduced. Tamoxifen was first injected during the early anagen of the first cycle as before, and a large piece of skin was excised when mice were aged 3 or 7 weeks. These particularly large wounds were previously shown to allow HF neogenesis within the healing wounds (Ito et al., 2007). Consistently, 19 days after wounding, de novo and unpigmented follicles were observed within the healing wounds (Supplementary Figure S6a–g) that produced white hairs

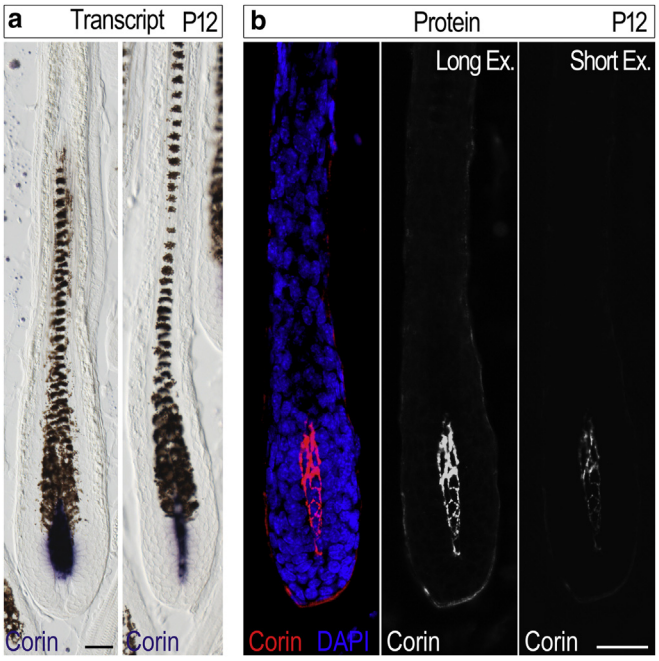

Figure 4. Corin levels in the DP and DSC are heterogeneous. (**a**) In situ hybridization for *Corin* is shown to illustrate that *Corin* transcripts (blue) are detected only within the DP. Two distinct types of follicles are displayed. n = 3 mice. Bar = 25 μm. (**b**) Immunostaining for Corin is shown to demonstrate the heterogeneity of Corin protein levels in the DP and DSC. The same follicle is presented in all panels. In the left panel, the channels for DAPI (blue) and Corin (red) are overlayed. In the middle and right panels, only the channel for Corin is shown in white to increase contrast and sensitivity. In the right panel, short exposure was used to illustrate the gradient pattern of Corin proteins in the DP and the heterogeneous levels of Corin within the DSC. n = 3 mice. Bar = 25 μm. DP, dermal papilla; DSC, dermal sheath cup; Ex, exposure; P, postnatal day.

(Supplementary Figure S6h and i). Remarkably, GFP-labeled cells detach from their follicle compartments and migrate toward the site of wound, suggesting that DS/DP cells contribute to wound healing (Figure 6a–i). The path of migration appears largely within the newly formed upper dermis in close proximity to the newly formed epidermis (Figure 6g and i). Whereas the current labeling method cannot distinguish between DS and DP cells and thus precludes further analysis of the precise origin of these migrating cells, DS cells leaving the DS compartment were clearly observed (Figure 6g and h). In contrast, GFP-labeled cells could not be detected within the DP or the DS of de novo follicles formed within the site of wound (Supplementary Figure S6j), suggesting that DP/DS cells originated from existing follicles at the boundaries of the wound do not contribute directly to de novo follicle formation during neogenesis.

DISCUSSION

In this study, we used the Corin-creRT2 line to specifically label DS cells in the DSC and provided clear evidence that hfDSCs are relocated from directly lining the DP during telogen to enveloping the matrix of the bulb region during anagen. Although this labeling method allows us to confirm and complement previous studies that used the aSMA-creRT2 line to label DS cells (González et al., 2017; Rahmani et al., 2014; Shin et al., 2020), differences are also apparent when the outcomes of the two labeling methods are compared. DS cells labeled by the aSMA driver tend to be evenly distributed within the middle region of the follicle. In contrast, DS cells labeled by the Corin driver preferentially reside in more proximal regions of the DS compartment. Furthermore, whereas the number of hfDSCs in the aSMA-driven lineage analysis decreases during aging, the number of hfDSCs in the Corin-driven labeling method is maintained. Finally, DS cells labeled by the aSMA driver contribute to follicle neogenesis during wound healing (Abbasi et al., 2020), whereas labeled DS cells by the Corin driver migrate toward the wound but do not participate in de novo follicle formation.

One possible mechanism to explain these discrepancies is that the labeling method used in this study preferentially marks hfDSCs with high capacity to self-renew, which results in the increase of the number of labeled hfDSCs from cycle to cycle. This not only explains the increase of labeled DS cells in the DDS from cycle to cycle but also provides a mechanistic insight into the maintenance of hfDSCs during aging observed in our study. Although stem cell exhaustion still occurs as previously reported (Shin et al., 2020), it is masked by the self-renewing capacity of hfDSCs. Furthermore, the existence of stem cell hierarchy within the DS compartment, which resembles the hierarchy that exists between bulge stem cells and the primed stem cells in the secondary germ of the follicular epithelium, is also a possibility underlying the differences between the two labeling methods. Whereas the aSMA-based labeling method labels a subpopulation within this hierarchy, the Corin-based method of labeling marks a different subpopulation of cells with different features. It is tempting to speculate that hfDSCs in the DSC that express high levels of Corin and low levels of aSMA are responsible for the long-term maintenance of the DS compartment, infrequently cycle, and are persistently relocated during anagen to the proximal part of the follicle where their stemness properties are maintained. In contrast, hfDSCs with reduced levels of Corin and elevated levels of aSMA descend from the Corin-high cells, frequently cycle, are relatively short lived, and are preferentially responsible for the expansion of the DS during regeneration. Methods that directly label hfDSCs are required to test this hypothesis.

The contribution of the DS to the maintenance of the dermis was previously speculated (Jahoda, 2003; Tobin et al., 2003a). Using the Corin-cerRT2 mouse line, we clearly show that such contribution does not occur during homeostasis throughout life. However, these boundaries between the mesenchymal components of the follicle and the dermis are perturbed during wound healing. Although the role of this cellular migration in contributing to wound healing and follicle neogenesis remains to be elucidated in future studies, our findings show that these migratory cells do not directly contribute to the formation of new DP or DS in the newly formed follicles within the wound and thus suggest that follicle neogenesis during wound healing is a

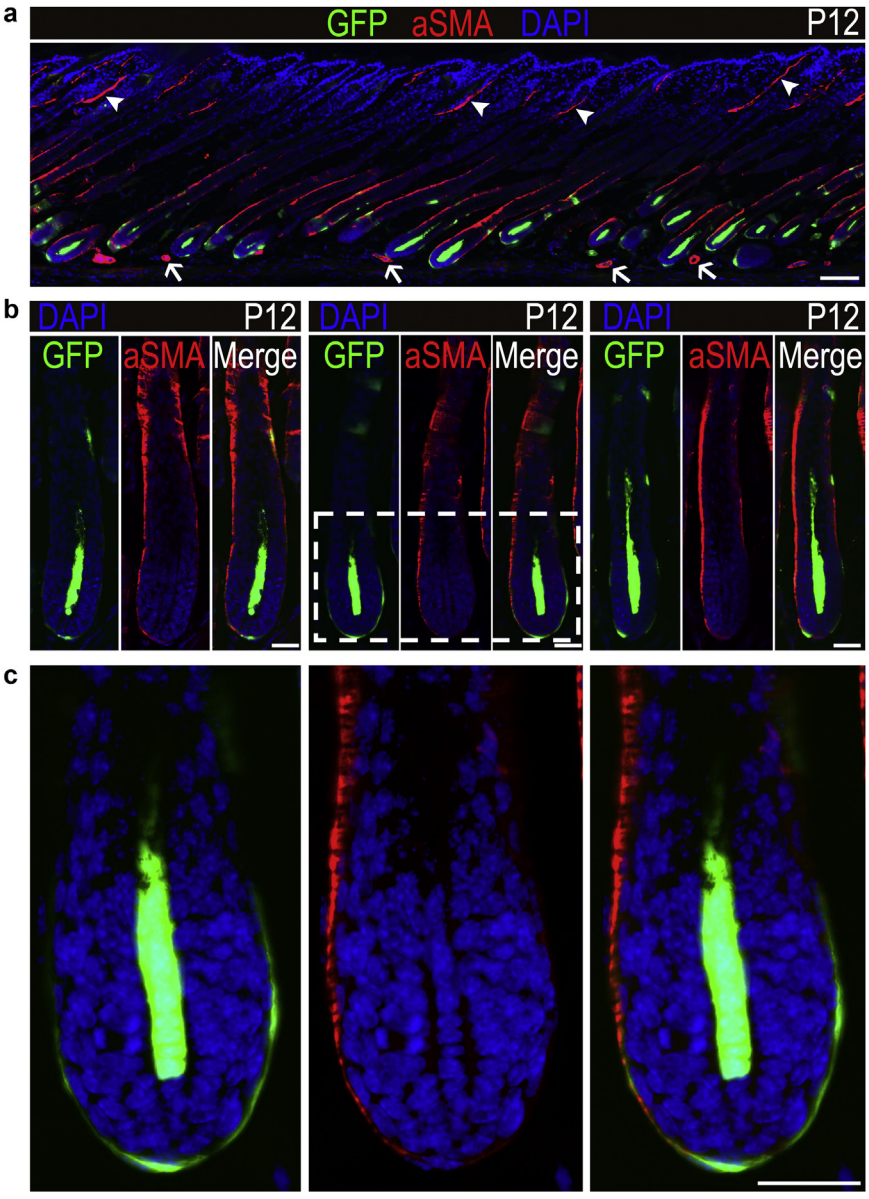

Figure 5. Induced GFP labeling in the DSC predominantly occurs in cells with low levels of aSMA. (**a**) Skin sections from tamoxifen-injected mice 2 days after injection (P12) were used for immunostaining of aSMA (red). n = 5 mice. Note that higher levels of aSMA in the DS are detected in the middle part of the follicle and that aSMA expression is asymmetric with higher levels in the anterior side of the follicle. In addition, aSMA is also expressed in the arrector pili muscle (white arrowheads) and the smooth muscle layer of blood vessels (white arrows). Bar = 100 μm. (**b**) Higher magnifications of three single follicles are shown to demonstrate that GFP-labeled cells within the DSC often express low levels of aSMA. Note the higher levels of aSMA in the anterior side of the DSC. For every single follicle, merged (right panel) and single channels for aSMA (middle panel) and GFP (left panel) are displayed. Bar = 25 μm. (**c**) A higher magnification of the field framed within the white dashed rectangle in **b** is presented. Bar = 25 μm. aSMA, alpha-smooth muscle actin; DS, dermal sheath; DSC, dermal sheath cup; P, postnatal day.

genuine de novo process of follicle formation not relying on pre-existing components imported from pre-existing follicles. Whereas YFP-positive cells labeled by aSMA-creRT2 were recently detected in both the DS and DP of newly formed follicles during wound healing (Abbasi et al., 2020), it is important to note however that aSMA is also expressed in smooth muscle cells of blood vessels, and the labeled cells in the DP/DS observed during neogenesis in that study do not necessarily originate from the DS of pre-existing follicles.

MATERIALS AND METHODS

Mice

A knock-in mouse line (Corin-CreRT2) expressing the inducible cre recombinase (i.e., CreRT2) specifically in the DP and DSC was generated by inserting CreRT2 in the *Corin* locus. Ai6 (RCL-ZsGreen) mice (Madisen et al., 2010) (having a GFP-variant allele, downstream to a floxed stop sequence, inserted in *Rosa26* locus) were obtained from the Jackson Laboratory (Bar Harbor, ME) and were used as a cre-reporter line. For cell lineage tracing, mice homozygous for the *Corin-CreRT2* allele and heterozygous for the r26EGFP reporter allele were generated. CreRT2 activity was induced by tamoxifen administration. All animal protocols were approved by the Institutional Animal Care and Use Committee at Bar-Ilan University (Safed, Israel).

Tamoxifen administration and skin sample processing

To induce CreRT2 activity, tamoxifen (Sigma-Aldrich, Inc, St. Louis, MO) was prepared in corn oil and administered as previously reported (Chevalier et al., 2014). Briefly, tamoxifen was intraperitoneally injected (200 μg/g body weight) once a day for 3 days on P8, P9, and P10 (early anagen of the first cycle). Middle dorsal skin samples were collected at multiple timepoints after labeling as indicated in the main text. Immediately after harvesting, skin

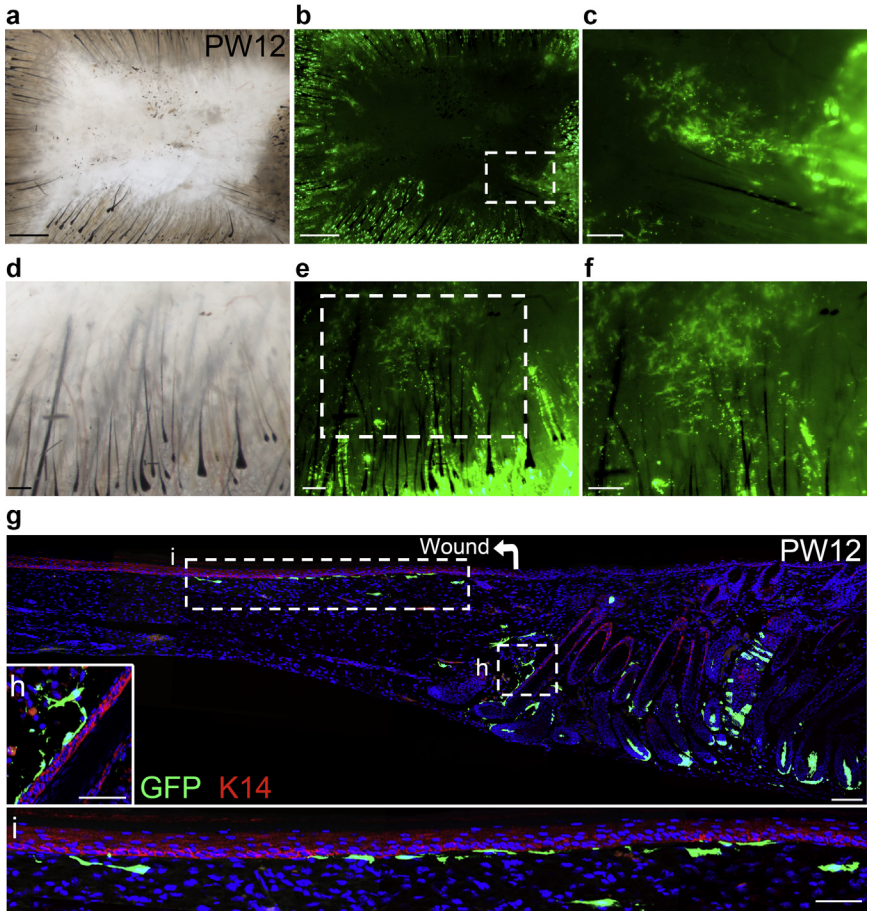

Figure 6. DS/DDS cells during wound healing exit the boundaries of the follicle and migrate to the wound area. Tamoxifen-injected mice aged 3 weeks were subjected to full-thickness back skin wounds. On PW12, the mice were killed, and the healing wounds were examined (**a–f**) by whole-mount imaging from the dermis side or (**g–i**) by serial cryosectioning and immunostaining. n = 5 mice. (**a**) Whole-mount brightfield and (**b**) fluorescent imaging of the same wound is shown. Bar = 1 mm. (**c**) Higher magnification of the white rectangle enclosed area in **b** is shown to demonstrate the groups of GFP-labeled migrating cells (green) within the wound. Bar = 200 μm. (**d**) Whole-mount brightfield and (**e**) fluorescent imaging of a different wound are shown. In **f**, a higher magnification of the white rectangle enclosed area in **e** is presented. Bar = 200 μm. (**g–i**) Healing wounds were sectioned to better examine the migratory path of the GFP-labeled cells. In all sections, the epidermis and ORS were labeled with anti-K14 (red), and DAPI labels the nuclei (blue). The wound area in **g** is indicated with the bent white arrow. Bar = 100 μm. Both **h** and **i** panels in the left side of and below **g** panel, respectively are higher magnifications of the white rectangle enclosed areas in **g**. Bar = 50 μm. Note that in **h**, GFP-positive cells detach from the DDS, and in **i**, the migratory path of GFP-labeled cells is in close proximity to the newly formed epidermis. Whole-wound images in **a–f** were taken using a fluorescent stereomicroscope, and sections in **g–i** were imaged using an upright fluorescence apotome microscope. DS, dermal sheath; DDS, distal dermal sheath; K14, keratin 14; ORS, outer root sheath; PW12, postwound day 12.

samples were fixed in 4% paraformaldehyde in PBS, dehydrated in sucrose solutions, embedded in optimal cutting temperature compound, frozen on liquid nitrogen, and cut into 10–12 μm frozen sections using a CM3050S Leica cryostat (Leica Microsystems, Wetzlar, Germany).

Depilation

To shorten and synchronize the telogen of the second and successive cycles, anagen was induced artificially by depilation. About a week after entering telogen, mice were anesthetized with tribromomethanol (0.6 mg/g body weight; Sigma-Aldrich, Inc); their dorsal hair coat was first clipped and then topped with warm wax and stripped after hardening. Hair growth was followed throughout the anagen phase to monitor the time follicles enter telogen, and 1 week later, depilation was repeated.

Wounding

As before, tamoxifen was intraperitoneally injected during the early anagen of the first cycle to label the DP and DSC, and full-thickness excision of dorsal skin was introduced when the mice were aged 3 or 7–8 weeks as previously described (Ito et al., 2007). Briefly, after anesthesia with tribromomethanol (0.6 mg/g body weight), 1 or 2.25 cm^2 of full-thickness skin was excised from mice aged 3 or 7–8 weeks, respectively. Healing wounds were collected at multiple timepoints after wounding as indicated in the main text.

TUNEL staining

Skin sections (10 μm) were washed twice with PBS, fixed with 4% paraformaldehyde for 10 minutes, and again washed twice with PBS 0.1% Tween. Subsequently, sections were incubated with proteinase K (10 μg/ml) for 5 minutes and washed twice with PBS 0.1% Tween. For TUNEL staining, the In Situ Cell Death Detection Kit-TMR red (Roche, Basel, Switzerland) was used according to the manufacturer's instructions. Briefly, 50 μl enzyme solution mixed in 550 μl label solution was applied on the sections, incubated for 60 minutes at 37 °C in a dark humidified box. Slides were washed three times in PBS before mounting with DAPI Fluoromount-G (Electron Microscopy Sciences, Hatfield, PA).

Immunofluorescence

Immunostaining was performed on frozen sections, which were fixed with 4% paraformaldehyde for 10 minutes, then washed three times with PBS for 5 minutes before blocking with 10% heat-inactivated sheep serum in PBS and 0.05% Tween solution for 2 hours, all done at room temperature. Sections were incubated with primary antibodies overnight at 4 °C and then washed with PBS three times for 5 minutes and incubated with secondary antibodies for 1 hour at room temperature. Excess antibodies were washed again with PBS three times for 5 minutes; sections were dried and mounted with DAPI Fluoromount-G. Both primary and secondary antibodies were diluted in 10% heat-inactivated sheep serum in PBS.

Primary antibodies used were guinea pig anti−keratin 14 antibodies (1:500; BioLegend, formerly Covance, Dedham, MA), rabbit anti−Perilipin-1 (1:200; Abcam, Cambridge, United Kingdom), rabbit anti−Caveolin-1 (1:250; Cell signaling technology, Danvers, MA), rabbit anti-aSMA (1:200; Sigma-Aldrich, Inc), goat anti-ITGA8 (1:20; R&D Systems, Minneapolis, MN), and rabbit anti-Corin (Enshell-Seijffers et al., 2008). Secondary antibodies used were donkey anti−guinea pig Cy5 (1:500; Jackson ImmunoResearch, West Grove, PA), donkey anti−rabbit TRITC (1:1,000; Jackson ImmunoResearch), and donkey anti−goat 647 (1:400; Jackson ImmunoResearch).

Imaging

For all section imaging, sections were mounted with DAPI Fluoromount-G. Images were acquired as stated in the text and figure legends using the Zeiss LSM780 inverted confocal microscope, the Zeiss Upright AxioImagerM2, and the Zeiss Upright fluorescent Apotom microscope. For whole-mount wound imaging, the Zeiss Discovery V12 fluorescent stereomicroscope was used. To acquire long fields of skin sections, the Zeiss Upright AxioImagerM2 was used through a ×20 objective with tiling and stitching mode. Image processing was performed with Adobe Photoshop CS5.1 (Adobe, San Jose, CA).

Data availability statement

No large datasets were generated or analyzed during this study.

ORCIDs

Emil Aamar: http://orcid.org/0000-0001-7924-4021
Efrat Avigad Laron: http://orcid.org/0000-0001-8502-6768
Wisal Asaad: http://orcid.org/0000-0002-2804-6313
Sarina Harshuk-Shabso: http://orcid.org/0000-0002-1023-6127
David Enshell-Seijffers: http://orcid.org/0000-0002-8228-2659

CONFLICT OF INTEREST

The authors state no conflict of interest.

ACKNOWLEDGMENTS

This research was funded by the Israel Science Foundation (1304/14). We thank Basem Hijazi for statistical assistance and Hofesh Haruach for technical support.

AUTHOR CONTRIBUTIONS

Conceptualization: DES; Formal Analysis: EA, WA; Funding Acquisition: DES; Investigation: EA, EAL, SHS, WA; Methodology: EA, EAL, DES, WA; Writing − Original Draft Preparation: EA, DES; Writing − Review and Editing: EA, DES

SUPPLEMENTARY MATERIAL

Supplementary material is linked to the online version of the paper at www.jidonline.org, and at https://doi.org/10.1016/j.jid.2021.05.023

REFERENCES

Abbasi S, Sinha S, Labit E, Rosin NL, Yoon G, Rahmani W, et al. Distinct regulatory programs control the latent regenerative potential of dermal fibroblasts during wound healing [published correction appears in Cell Stem Cell 2021;28:581−3]. Cell Stem Cell 2020;27:396−412.e6.

Avigad Laron E, Aamar E, Enshell-Seijffers D. The mesenchymal niche of the hair follicle induces regeneration by releasing primed progenitors from inhibitory effects of quiescent stem cells. Cell Rep 2018;24:909−21.e3.

Botchkarev VA, Kishimoto J. Molecular control of epithelial-mesenchymal interactions during hair follicle cycling. J Investig Dermatol Symp Proc 2003;8:46−55.

Chevalier C, Nicolas JF, Petit AC. Preparation and delivery of 4-hydroxy-tamoxifen for clonal and polyclonal labeling of cells of the surface ectoderm, skin, and hair follicle. Methods Mol Biol 2014;1195:239−45.

Chi W, Wu E, Morgan BA. Dermal papilla cell number specifies hair size, shape and cycling and its reduction causes follicular decline. Development 2013;140:1676−83.

Chi WY, Enshell-Seijffers D, Morgan BA. De novo production of dermal papilla cells during the anagen phase of the hair cycle. J Invest Dermatol 2010;130:2664−6.

Enshell-Seijffers D, Lindon C, Kashiwagi M, Morgan BA. Beta-catenin activity in the dermal papilla regulates morphogenesis and regeneration of hair. Dev Cell 2010a;18:633−42.

Enshell-Seijffers D, Lindon C, Morgan BA. The serine protease Corin is a novel modifier of the Agouti pathway. Development 2008;135:217−25.

Enshell-Seijffers D, Lindon C, Wu E, Taketo MM, Morgan BA. Beta-catenin activity in the dermal papilla of the hair follicle regulates pigment-type switching. Proc Natl Acad Sci USA 2010b;107:21564−9.

González R, Moffatt G, Hagner A, Sinha S, Shin W, Rahmani W, et al. Platelet-derived growth factor signaling modulates adult hair follicle dermal stem cell maintenance and self-renewal. NPJ Regen Med 2017;2:11.

Harshuk-Shabso S, Dressler H, Niehrs C, Aamar E, Enshell-Seijffers D. Fgf and Wnt signaling interaction in the mesenchymal niche regulates the murine hair cycle clock. Nat Commun 2020;11:5114.

Heitman N, Sennett R, Mok KW, Saxena N, Srivastava D, Martino P, et al. Dermal sheath contraction powers stem cell niche relocation during hair cycle regression. Science 2020;367:161−6.

Hsu YC, Pasolli HA, Fuchs E. Dynamics between stem cells, niche, and progeny in the hair follicle. Cell 2011;144:92−105.

Ito M, Kizawa K, Hamada K, Cotsarelis G. Hair follicle stem cells in the lower bulge form the secondary germ, a biochemically distinct but functionally equivalent progenitor cell population, at the termination of catagen. Differentiation 2004;72:548−57.

Ito M, Yang Z, Andl T, Cui C, Kim N, Millar SE, et al. Wnt-dependent de novo hair follicle regeneration in adult mouse skin after wounding. Nature 2007;447:316−20.

Jahoda CA. Cell movement in the hair follicle dermis - more than a two-way street? J Invest Dermatol 2003;121:ix−xi.

Kaushal GS, Rognoni E, Lichtenberger BM, Driskell RR, Kretzschmar K, Hoste E, et al. Fate of prominin-1 expressing dermal papilla cells during homeostasis, wound healing and Wnt activation. J Invest Dermatol 2015;135:2926−34.

Legué E, Nicolas JF. Hair follicle renewal: organization of stem cells in the matrix and the role of stereotyped lineages and behaviors. Development 2005;132:4143−54.

Madisen L, Zwingman TA, Sunkin SM, Oh SW, Zariwala HA, Gu H, et al. A robust and high-throughput Cre reporting and characterization system for the whole mouse brain. Nat Neurosci 2010;13:133−40.

Martino PA, Heitman N, Rendl M. The dermal sheath: an emerging component of the hair follicle stem cell niche. Exp Dermatol 2021;30:512−21.

McElwee KJ, Kissling S, Wenzel E, Huth A, Hoffmann R. Cultured peribulbar dermal sheath cells can induce hair follicle development and contribute to the dermal sheath and dermal papilla. J Invest Dermatol 2003;121:1267−75.

Mesa KR, Rompolas P, Zito G, Myung P, Sun TY, Brown S, et al. Niche-induced cell death and epithelial phagocytosis regulate hair follicle stem cell pool. Nature 2015;522:94−7.

Millar SE. Molecular mechanisms regulating hair follicle development. J Invest Dermatol 2002;118:216−25.

Plikus MV, Mayer JA, de la Cruz D, Baker RE, Maini PK, Maxson R, et al. Cyclic dermal BMP signalling regulates stem cell activation during hair regeneration. Nature 2008;451:340−4.

Rahmani W, Abbasi S, Hagner A, Raharjo E, Kumar R, Hotta A, et al. Hair follicle dermal stem cells regenerate the dermal sheath, repopulate the dermal papilla, and modulate hair type. Dev Cell 2014;31:543–58.

Rompolas P, Deschene ER, Zito G, Gonzalez DG, Saotome I, Haberman AM, et al. Live imaging of stem cell and progeny behaviour in physiological hair-follicle regeneration. Nature 2012;487:496–9.

Shin W, Rosin NL, Sparks H, Sinha S, Rahmani W, Sharma N, et al. Dysfunction of hair follicle mesenchymal progenitors contributes to age-associated hair loss. Dev Cell 2020;53:185–98.e7.

Stenn KS, Paus R. Controls of hair follicle cycling. Physiol Rev 2001;81:449–94.

Tao Y, Yang Q, Wang L, Zhang J, Zhu X, Sun Q, et al. β-Catenin activation in hair follicle dermal stem cells induces ectopic hair outgrowth and skin fibrosis. J Mol Cell Biol 2019;11:26–38.

Tobin DJ, Gunin A, Magerl M, Handijski B, Paus R. Plasticity and cytokinetic dynamics of the hair follicle mesenchyme: implications for hair growth control. J Invest Dermatol 2003a;120:895–904.

Tobin DJ, Gunin A, Magerl M, Paus R. Plasticity and cytokinetic dynamics of the hair follicle mesenchyme during the hair growth cycle: implications for growth control and hair follicle transformations. J Investig Dermatol Symp Proc 2003b;8:80–6.

Yang H, Adam RC, Ge Y, Hua ZL, Fuchs E. Epithelial-mesenchymal micro-niches govern stem cell lineage choices. Cell 2017;169:483–96.e13.

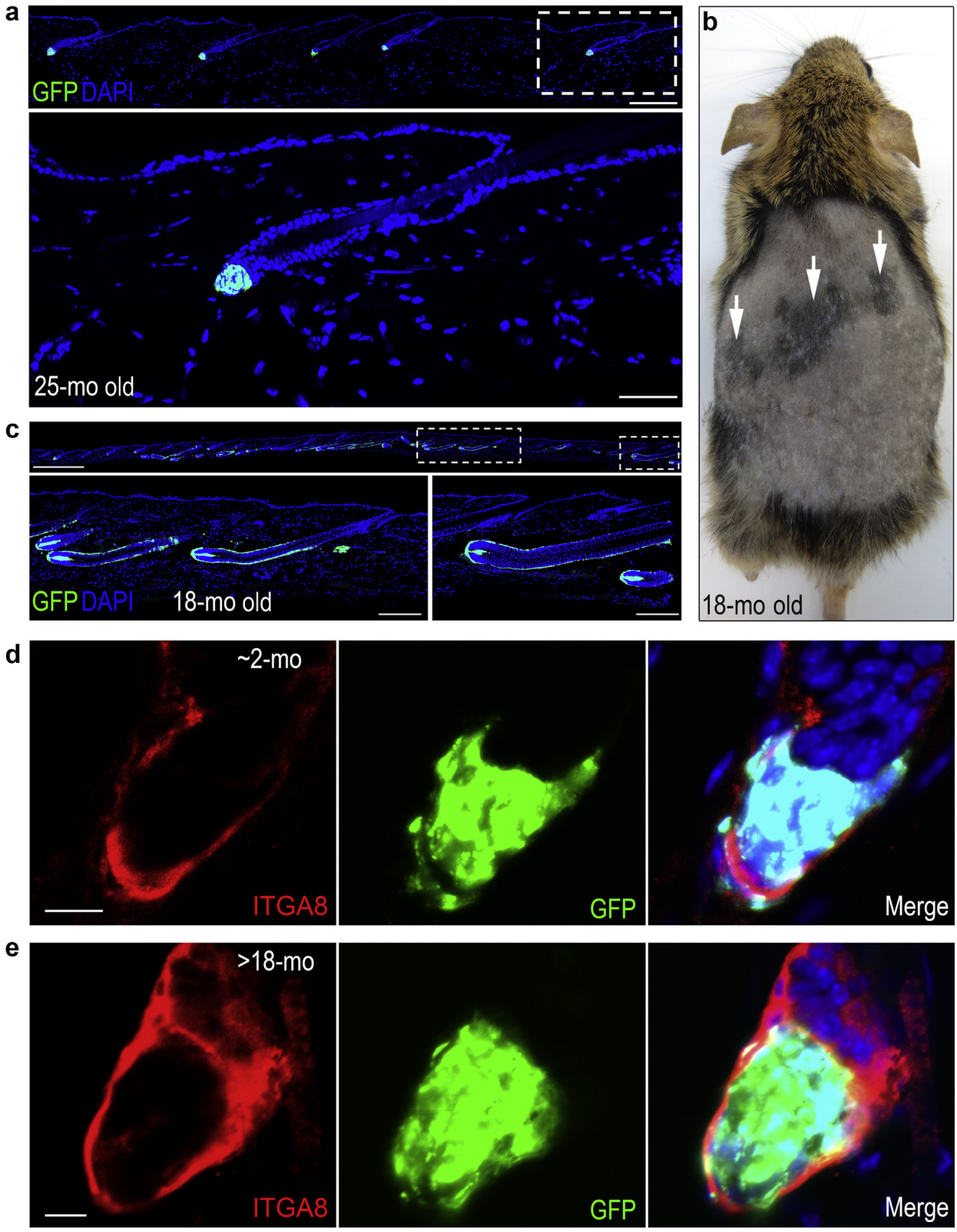

Supplementary Figure S1. GFP-labeled cells in aged mice remain restricted to the DP and DS. (**a**) A skin section of a tamoxifen-injected, undepilated mouse aged 25 mo at telogen is fluorescently imaged to demonstrate the confined expression of GFP (green) to the DP/DS compartments. n = 5 mice. Bar = 200 μm. Higher magnification of the field enclosed in the white dashed rectangle is shown in the panel below. Bar = 50 μm. (**b**) A tamoxifen-injected, undepilated mouse aged 18 mo after hair coat clipping is shown to demonstrate the patches of spontaneous anagen (white arrows). (**c**) A cross-section through the anagen patch of the mouse in **b** is displayed to illustrate GFP expression (green) in the DS. Bar = 1 mm. The lower panels present higher magnifications of the fields framed within the white dashed rectangles in the upper panel. Bar = 200 μm. n = 4 mice. Telogen follicles from (**d**) a mouse aged ~2 mo and from (**e**) a mouse aged >18 mo are shown to illustrate GFP-labeled DS cells. Left, middle, and right panels are images of the same follicle showing ITGA8 immunostaining on the left (red), GFP in the middle (green), and a merge on the right. Bar = 10 μm. DP, dermal papilla; DS, dermal sheath; mo, month.

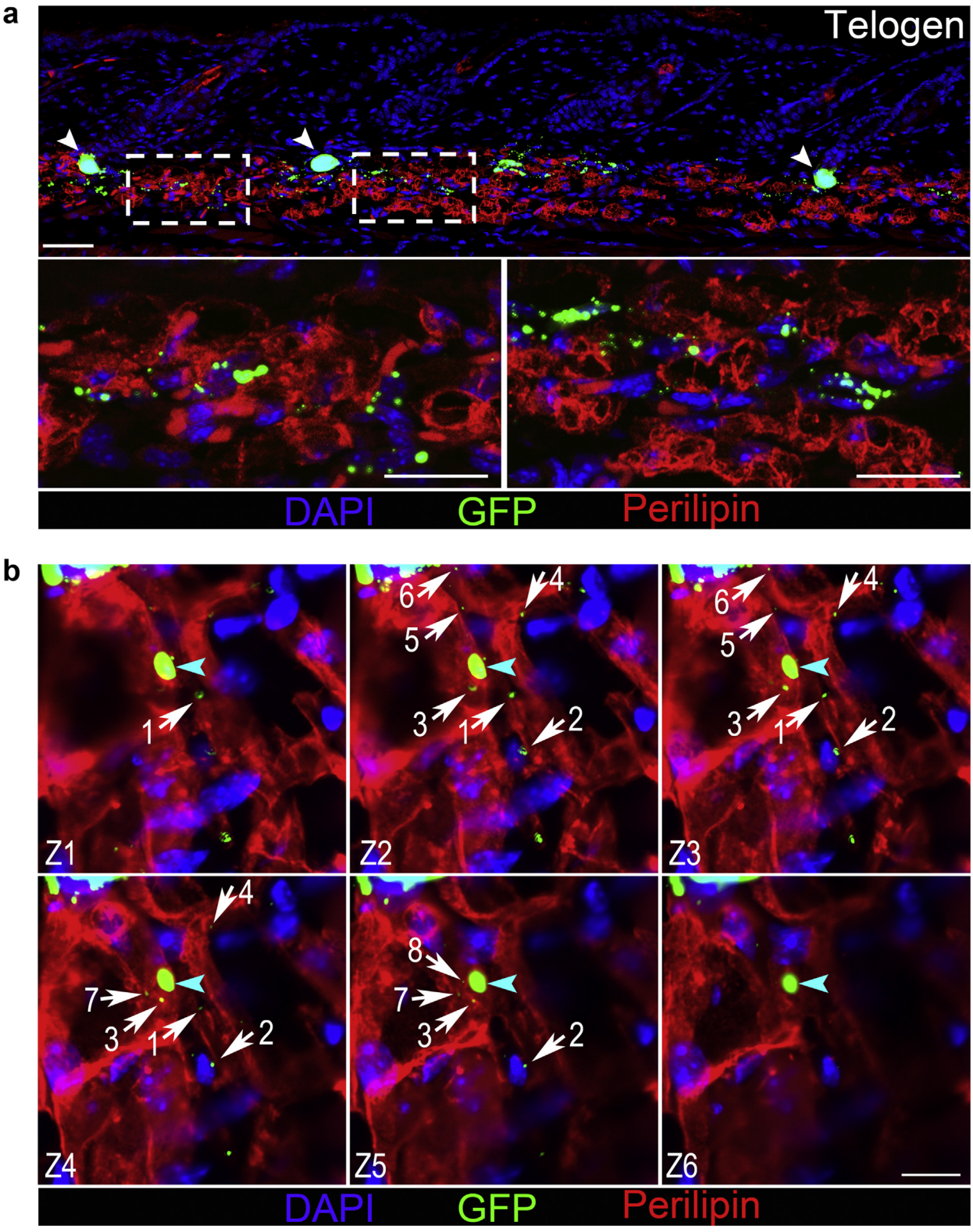

Supplementary Figure S2. GFP-labeled cellular fragments are internalized by adipocytes. Tamoxifen-injected mice were examined at the telogen phase. (**a**) Skin samples of the first telogen were cryosectioned and immunostained with anti-Prelipin (red), a specific marker for mature adipocytes. The GFP-labeled fragments (green) colocalize with the panniculus adiposus layer (red). Arrowheads indicate GFP-labeled DPs. Bar = 100 μm. The lower panels show higher magnifications of the selected fields enclosed with white dashed rectangles in the upper panel. Bar = 25 μm. All images show colocalization of some of the GFP-labeled remnants with the perilipin-stained adipocyte cells. DAPI labels the nuclei (blue). Images were captured using an upright apotome microscope. n = 3 mice. (**b**) Serial optical sections (Z1–Z6), acquired by Z-stack confocal imaging, are shown to illustrate the colocalization of the GFP fragments (green) with the adipocyte marker perilipin (red). A cyan arrowhead indicates a large GFP fragment that is detected throughout all sections, whereas the numbered white arrows indicate small GFP fragments that are observed in only some of the optical sections. Bar = 10 μm. DP, dermal papilla.

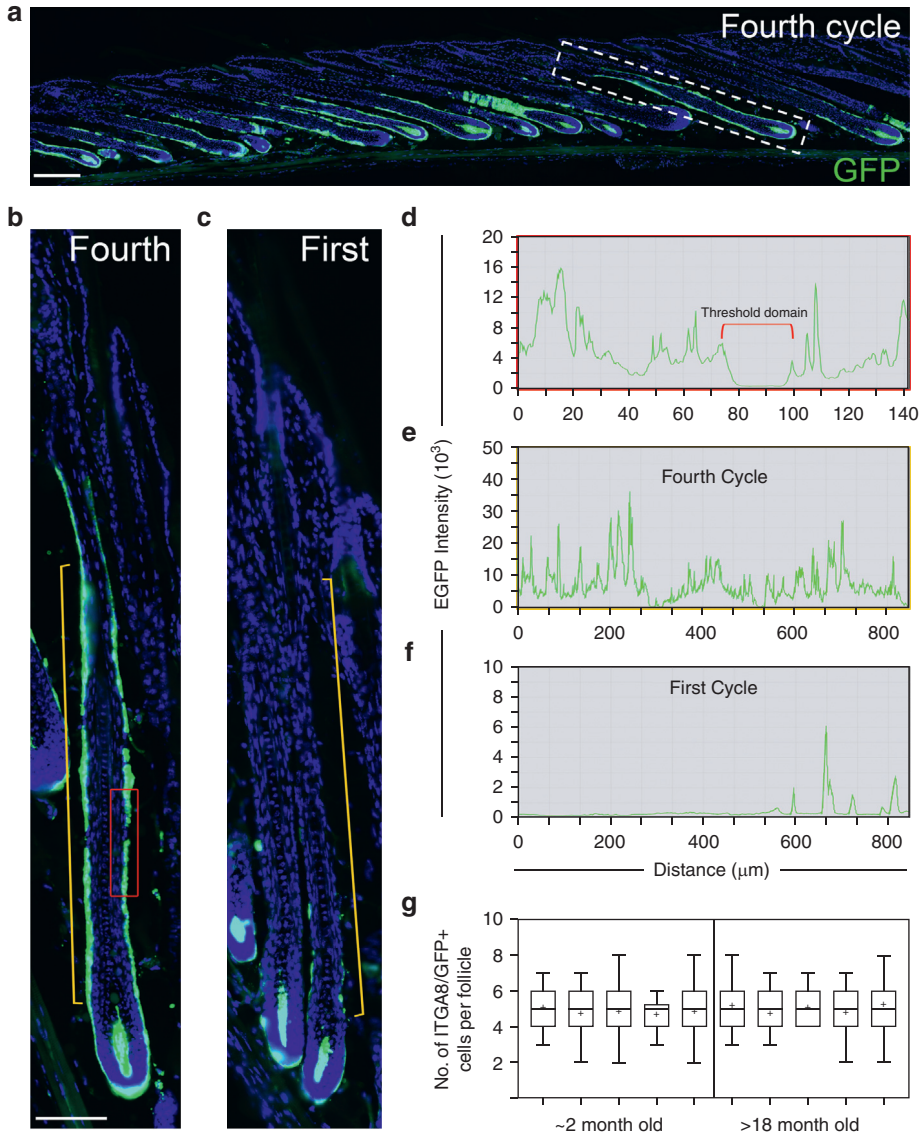

Supplementary Figure S3. Cell lineage quantification of GFP labeling. Methodology to quantify the ratio between GFP-labeled to -unlabeled DDS compartment is illustrated in **a**–**f**. Quantification of labeled hfDSCs per follicle during telogen in young and old individual mice is presented in **g**. Skin samples of tamoxifen-injected mice were examined during the anagen stage of four consecutive cycles and during the telogen stage of young and old mice. (**a**) Anagen skin section of the fourth cycle, showing expanded domain of GFP expression along the DDS of the hair follicle. Bar = 200 μm. (**b**) Higher magnification of the follicle enclosed with a white dashed rectangle in **a**. The yellow bracket demarcates a fixed distance of 900 μm, in which the intensity of green fluorescence along this distance was measured in all follicles. The red rectangle on the right defines a domain (150 μm) in which a GFP-negative region flanked between GFP+ segments was used to define a value for a negative signal. Bar = 100 μm. (**c**) Follicles at the anagen phase of the first cycle are shown. (**d**) The GFP intensity values along the distance of the red rectangle in **b** are shown. The GFP-negative region is bracketed in red. Note that the intensities along this domain are <400 and represent the background. Therefore, 400 is the threshold value. (**e, f**) Examples of GFP intensities along the fixed distance of one follicle during the fourth and first cycles are shown, respectively, to illustrate the decline in GFP intensity from cycle to cycle. A progressive increase of labeled DS cells is observed in the DDS compartment from cycle to cycle, expanding distally from the DSC. (**g**) The number of labeled DS cells (ITGA8/GFP double positive) per telogen follicle in young (aged ~2 months) and old (aged >18 months) mice was individually quantified and presented as a box and whisker plot (midline: median, cross: mean, box: 25th and 75th percentiles, whiskers: minimum and maximum). At least 30 follicles per mouse were scored. DDS, distal dermal sheath; DSC, dermal sheath cup; hfDSC, hair follicle dermal stem cell; No., number.

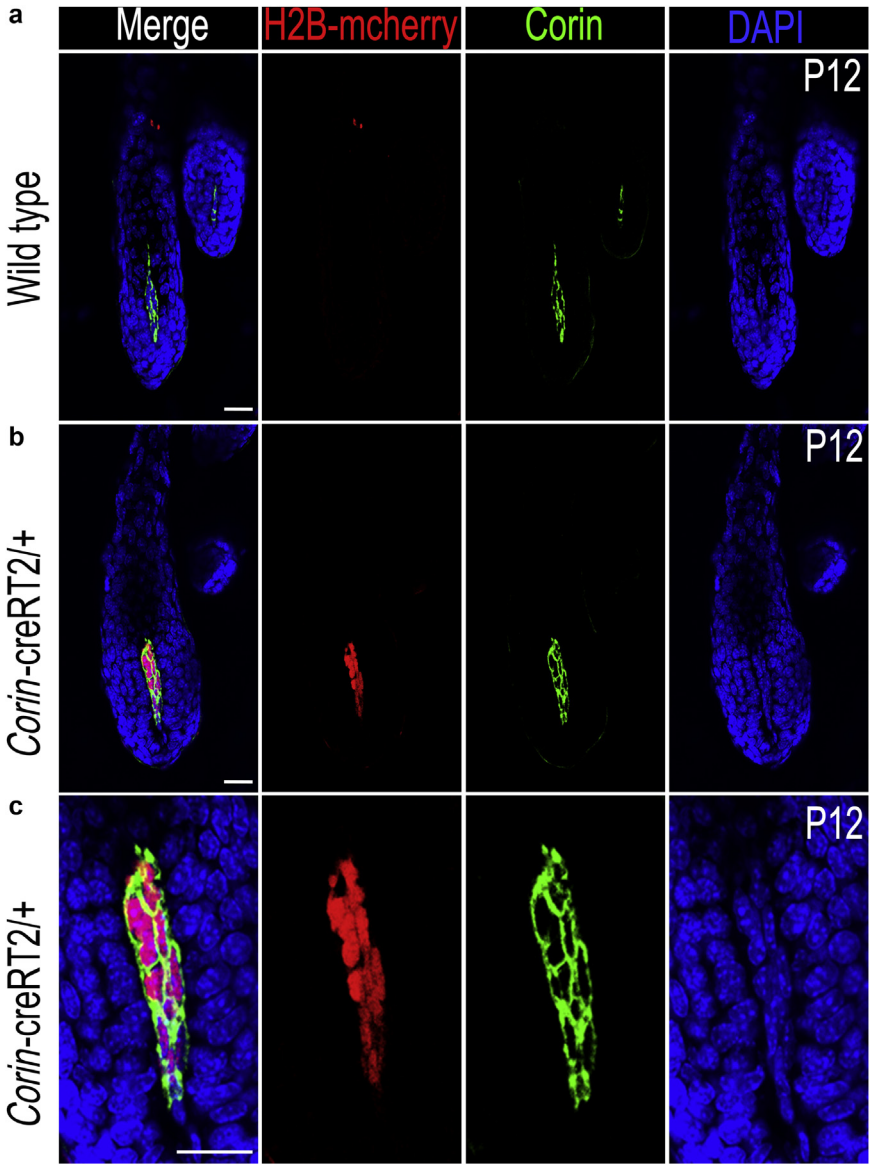

Supplementary Figure S4. mCherry-H2B expression in the *Corin*-creRT2 knock-in mouse line. The mCerry-H2B was inserted into the Corin locus upstream to the creRT2. (**a, b**) Fluorescent images of follicles from (**a**) a wild-type mouse and (**b**) a heterozygote for the knock-in allele are shown to demonstrate the nuclear expression of mCherry-H2B only in the knock-in mouse line without tamoxifen injection. Images of single channels for mCherry-H2B, Corin immunostaining, and DAPI are included and indicated accordingly. n = 3 mice per genotype. Bar = 20 μm. (**c**) Higher magnifications of the field around the DP in **b** are presented. Bar = 20 μm. DP, dermal papilla; P, postnatal day.

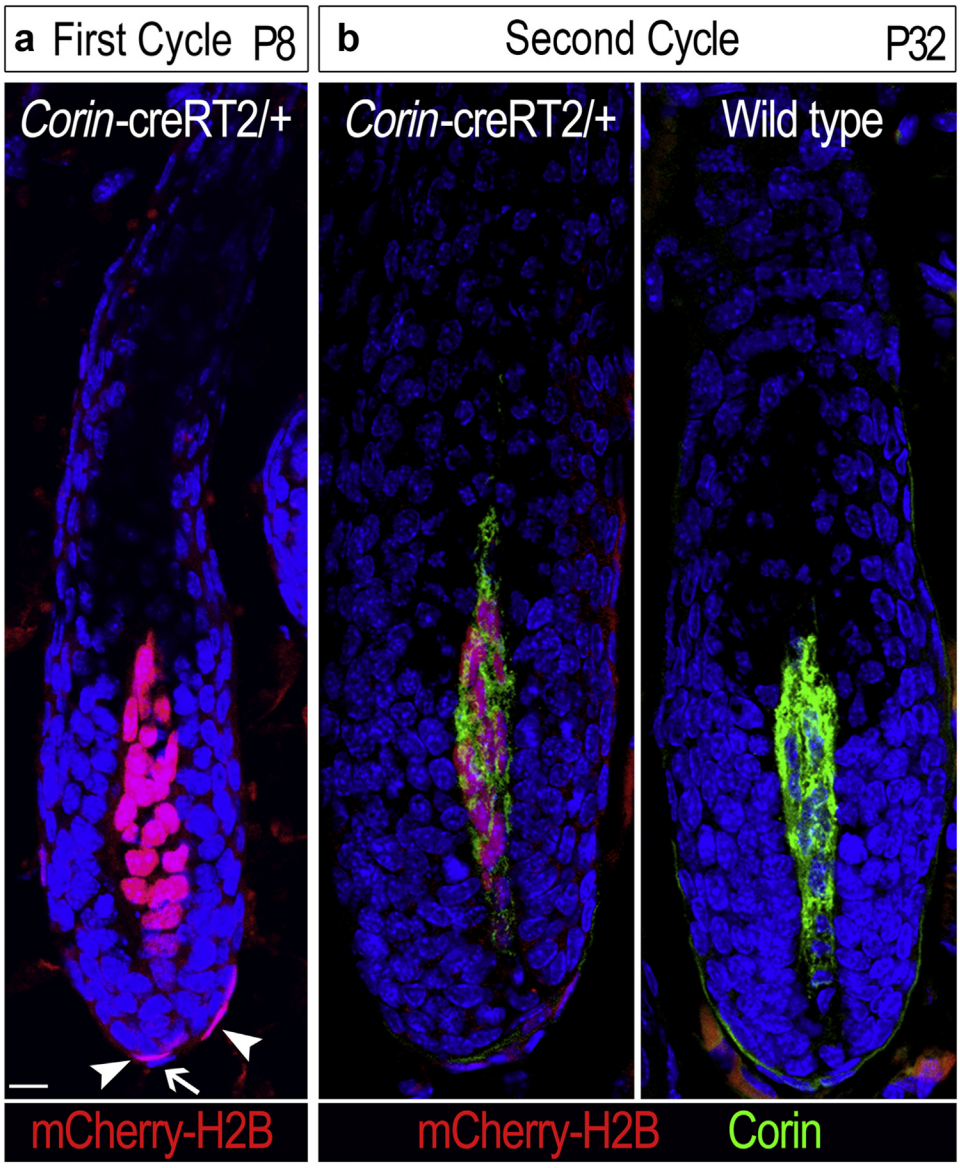

Supplementary Figure S5. mCherry-H2B expression driven by the *Corin* locus further corroborates Corin expression heterogeneity in the DP and DSC. (**a**) mCherry-H2B (red) fluorescence imaging of a follicle from a heterozygous mouse for the *Corin*-creRT2 allele during anagen of the first cycle (P8) is displayed. Note the gradient along the distal–proximal axis of the DP and the presence of both labeled (white arrowheads) and unlabeled (white arrow) DSC cells. n = 3 mice. (**b**) Corin immunostaining (green) and mCherry-H2B (red) fluorescent image of a single follicle from a heterozygous mouse for the *Corin*-creRT2 allele (left panel) and a wild-type mouse (right panel) during anagen of the second cycle (P32) is shown. Note that the image in **a** and the right image in **b** are overly exposed to illustrate the presence and absence of mCherry-H2B expression in the DSC, respectively. Nuclei are in blue (DAPI). n = 3 mice. Bar = 10 μm. DP, dermal papilla; DSC, dermal sheath cup; P, postnatal day.

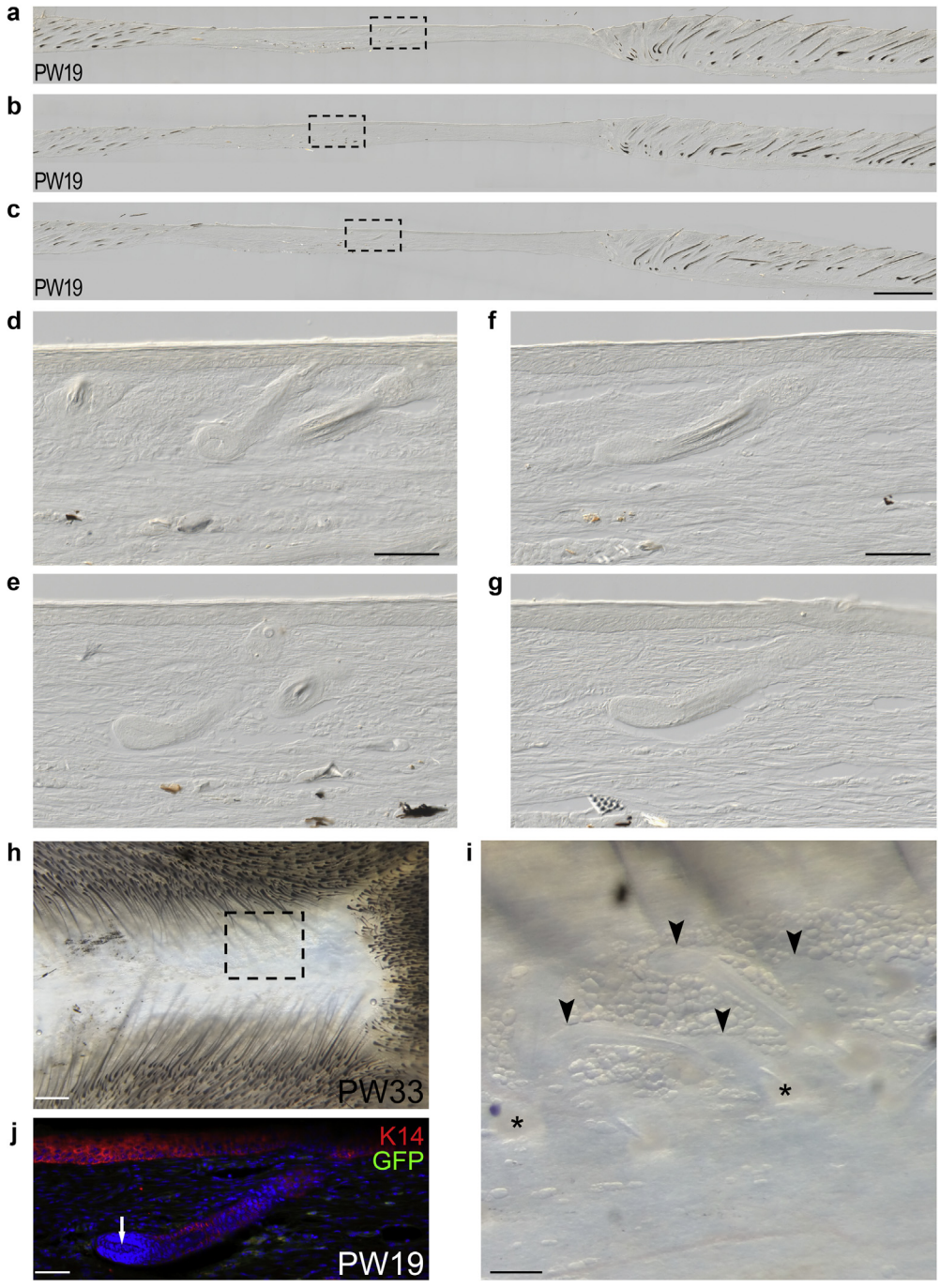

Supplementary Figure S6. Follicle neogenesis within the healing wound. Tamoxifen-injected mice during the early anagen of the first cycle were subjected to full-thickness 1 cm square skin wounds when they were aged 3 weeks. (**a–c**) Three alternate sections derived from the same wound on PW19 are imaged by DIC microscopy and shown to illustrate de novo follicle formation within the wound. Note the pigmented mid-anagen follicles at the periphery of the wound. n = 5 mice. Bar = 1 mm. (**d, e**) Higher magnifications of the fields within the black dashed rectangles in **a** and **b** are respectively displayed to demonstrate newly formed, unpigmented follicles, in sharp contrast to the pigmented, fully blown anagen follicles in the peripheries of the wound. Bar = 100 μm. (**f, g**) Higher magnifications of two serial sections from the field framed within the black dashed rectangle in **c** are presented. Bar = 100 μm. (**h**) An image of healed wound on PW33 is taken from the dermis side. Bar = 1 mm. (**i**) A higher magnification of the field enclosed within the dashed black rectangle in **h** is shown. Note the de novo and unpigmented follicles within the healing wound. Black stars indicate sebaceous glands, whereas arrowheads indicate bulb regions of some newly formed follicles. Bar = 200 μm. (**j**) Tamoxifen-injected mice during early anagen of the first cycle were subjected to full-thickness 2.5 cm square skin wounds when they were aged 7 weeks. Immunostaining with anti-K14 of a wound section reveals a newly formed hair follicle inside the wound on PW19. Nuclei were labeled with DAPI (blue). Note that neither the DP (arrow) nor the DS show any GFP expression. Whole-wound images were taken using a stereomicroscope, and sections were imaged using an upright fluorescence apotome microscope. n = 5 mice. Bar = 50 μm. DIC, differential interference contrast; DP, dermal papilla; DS, dermal sheath; K14, keratin 14; PW, postwound day.